On the Design of a Three-DOF Cable-Suspended Parallel Robot Based on a Parallelogram Arrangement of the Cables

Dinh-Son Vu, Eric Barnett, Anne-Marie Zaccarin, and Clément Gosselin(✉)

Robotics Laboratory, Department of Mechanical Engineering,
Pavillon Adrien-Pouliot, Université Laval, Québec, QC G1V 0A6, Canada
{dinh-son.vu.1,eric.barnett.1,anne-marie.zaccarin.1}@ulaval.ca,
clement.gosselin@gmc.ulaval.ca

Abstract. An original design for a cable-suspended mechanism based on six cables, but actuated with three motors, is proposed in this paper. Each pair of cables is wound by a single actuator and their attachment points on the mobile platform and on the fixed base form a parallelogram, so that the orientation of the mobile platform remains constant while performing translational movements. First, the paper presents the architecture of the three-degree-of-freedom (three-DOF) manipulator and its corresponding kinematic equations. Then, the static workspace of the mechanism is determined analytically based on the simplification of the Jacobian matrix for a constant orientation of the mobile platform. Finally, the static workspaces of several cable arrangements are compared in order to assess the capabilities of the presented mechanism. In particular, one configuration of the three-DOF system with crossing cables is studied in more detail.

1 Introduction

Cable-driven parallel mechanisms offer numerous advantages compared to rigid-link robots, including large workspaces, high dynamic movement capabilities, effective payload-to-mass ratios, and ease of implementation. However, the inherent drawback of cable-driven robots is that cables cannot push on the moving platform; they can only exert pulling forces. Fully constrained end-effectors require $(n+1)$ cables in order to control n degrees of freedom. However, cable-suspended parallel robots use gravity in order to maintain cable tension, which acts similarly to a cable pulling downward. Therefore, the number of physical cables required to drive the effector is equal to the number of actuated degrees of freedom, assuming that some limitations on the platform accelerations are satisfied.

Workspace assessment is a critical step during cable mechanism design. Different approaches have been explored to determine the achievable positions of the mobile platform for different robot configurations. The static equilibrium workspace of a point-mass effector [1] gives all the positions for which the tension of all cables remains positive. Similarly, the constant orientation workspace

C. Gosselin et al. (eds.), *Cable-Driven Parallel Robots*,
Mechanisms and Machine Science 53, DOI 10.1007/978-3-319-61431-1_27

of a mobile platform, which has been studied for the Robocrane [2] and for a six-DOF cable-suspended robot [3], provides its possible positions for a given constant orientation, assuming positive cable tensions. The calculation of the interference-free workspace [4] examines the static workspace of cable robots while taking into account the possible contacts between the cables. The volume obtained by setting a maximum and minimum tension in the cables and a particular wrench load applied at the platform is defined as the wrench-feasible workspace [5–7] and its shape is a zonotope whose boundaries depend on the tension limits.

Examples of six-DOF cable mechanisms that control the movement of the end-effector in both translation and orientation can be found in [2,3,8]. However, in many tasks for which cable-suspended parallel mechanisms are potential candidates, only translational motions are required. For example, in [9], a six-DOF cable-driven robot comprising eight actuators is proposed for pick-and-place operations and in [10], a six-DOF cable-driven robot that uses six actuators is proposed for the 3D printing of large objects, an application that only requires translational motion at constant orientation. In such cases, it is advantageous to reduce the number of actuators to the number of degrees of freedom required at the platform. Therefore, similarly to what was done in [11–13], this paper introduces the design of a three-DOF cable-suspended mechanism for the three spatial translations with constant orientation of the end-effector. First, the possible geometric arrangements of the three-DOF mechanism are described. Then, the general kinematic modelling of a six-DOF cable-suspended mechanism and the analytical calculation of the equations defining its static workspace for constant platform orientation are derived. This general result is then applied to the particular architecture of the proposed three-DOF mechanism with the cables crossing over the platform. Finally, the static equilibrium workspace obtained with the three-DOF mechanism for a few different configurations is compared with the workspace of a six-DOF cable-suspended robot used for large-scale 3D printing [10].

2 Geometry of the Three-DOF Cable-Suspended Mechanism with Parallelogram Architecture

Six individually actuated cables are generally used to constrain the suspended mobile platform in the six spatial DOFs. However, as shown in [11–13], if only translations are needed with a constant orientation, cables can be arranged as parallelograms and driven using only three independent motors. However, the geometric arrangement of the parallelograms proposed in [11–13] is based on a "convergent" design, which significantly limits the static workspace, as it will be shown in this paper.

The architecture proposed in this paper is based on parallelograms but the geometry is inspired from that proposed in [8]. The cables are crossing over the moving platform, thereby increasing the workspace without inducing cable interferences. It should also be pointed out that cable-driven mechanisms using

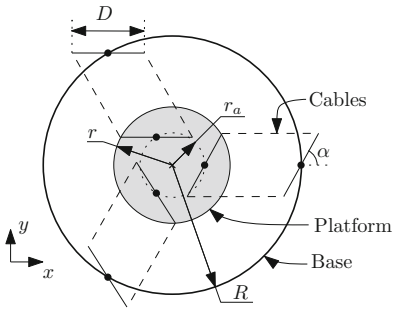

Fig. 1. Arrangement of the parallelograms based on the parallelogram width D, the orientation of the platform attachment points α and the distance to the attachment points relative to the centre of the moving platform r_a. The platform and the base are parallel horizontal planes at different elevations.

one motor to drive two parallel cables have also been proposed in the literature [14] in order to constrain *planar* cable-driven mechanisms to the plane of motion.

2.1 Architecture of the Three-DOF Mechanism

Figure 1 presents the parameters that are used to describe the geometry of the attachment points, and thus the arrangement of the parallelogram of each pair of cables driven by the same actuator. The parallelogram width (distance between two cables in a pair) and orientation are described by parameters D and α, respectively. Parameter r_a is the radius of the circle on the moving platform on which the midpoint of the line segment joining each pair of attachment points is placed. The size of the moving platform and the base are directly linked to the radii r and R respectively, which are primary design parameters that affect the footprint of the mechanism. Radius R corresponds to the circle on the base on which the centre of each pair of attachment points is located, while r is the radius of the smallest disk on the platform that includes all attachment points.

(a) Trivial architecture designed to avoid interference between cables.

(b) Architecture inspired by the geometry proposed in [8] for platforms with six actuators and crossing cables.

Fig. 2. Possible architectures of the three-DOF cable-suspended robot based on a parallelogram arrangement of the cables.

2.2 Example Architectures

The geometric parameters defined above strongly influence the achievable workspace and can be used to describe a broad variety of architectures [15]. Figure 2 shows two examples of possible architectures for a three-DOF cable-suspended mechanism based on a parallelogram arrangement of the cables, with the design parameters listed in Table 1. The trivial architecture shown in Fig. 2a avoids mechanical interference among the cables. This architecture corresponds to the design proposed in [11–13]. Crossing the cables over the mobile platform is known to increase the workspace of the mechanism, at the cost of potential interference among the cables [4,16]. However, by crossing only one cable of each pair that forms a parallelogram over the mobile platform, the static workspace of the robot can potentially be increased without generating this undesired interference. To maintain the parallelogram architecture, the fixed-frame cable attachment points must also be moved, as shown in Fig. 2b. This architecture, proposed here and inspired by that disclosed in [8], guarantees that there will be no cable-cable interference, a claim which can be proven by performing an analysis similar to that shown in [8] for a six-DOF robot.

Table 1. Parameters for the two architectures shown in Fig. 2. Position vector $\mathbf{b}_i$ goes from the centre of the platform to cable attachment point B_i, for the architecture with crossing cables, as shown in Fig. 3.

	r_a		D		α
Trivial architecture	$\frac{\sqrt{3}}{2}r$		r		$-\frac{\pi}{2}$
Architecture with crossing cables	0		$2r$		$-\frac{\pi}{3}$
$\mathbf{b}_1$	$\mathbf{b}_2$	$\mathbf{b}_3$	$\mathbf{b}_4$	$\mathbf{b}_5$	$\mathbf{b}_6$
$r[\frac{1}{2}, \frac{-\sqrt{3}}{2}, 0]^T$	$r[\frac{-1}{2}, \frac{\sqrt{3}}{2}, 0]^T$	$r[\frac{1}{2}, \frac{\sqrt{3}}{2}, 0]^T$	$r[\frac{-1}{2}, \frac{-\sqrt{3}}{2}, 0]^T$	$r[-1, 0, 0]^T$	$r[1, 0, 0]^T$

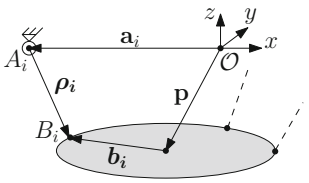

Fig. 3. Kinematic modelling of the cable platform.

3 Analytical Determination of the Static Workspace

The static equilibrium workspace corresponds to the set of positions of the moving platform for which the cables are in tension. Its analytical determination for constant orientation is based on the analysis of the Jacobian matrix of the manipulator.

3.1 Kinematic Modelling of a Six-DOF Cable-Suspended Robot

Even though the mechanism is actuated with only three motors, six cables transmit forces to the platform so the equations that describe the motion resemble those of a six-DOF cable-suspended mechanism. Figure 3 shows the notation used to establish the kinematic equations of the mechanism. For cable i, position vector $\mathbf{a}_i$ goes from the origin of the base frame to the base attachment point A_i, while position vector $\mathbf{b}_i$ goes from the centre of the platform (reference point) to the platform attachment point B_i. The position of the reference point of the moving platform with respect to the origin of the base frame is referred to as $\mathbf{p} = [x, y, z]^T$. The vector along cable i, connecting point A_i to point B_i is denoted $\boldsymbol{\rho}_i$. The relationship between vectors $\mathbf{a}_i$, $\mathbf{b}_i$, and $\boldsymbol{\rho}_i$ is as follows

$$\boldsymbol{\rho}_i = \mathbf{p} + \mathbf{b}_i - \mathbf{a}_i. \tag{1}$$

Since the orientation of the platform remains constant with respect to the base, the expression of the attachment points $\mathbf{a}_i$ and $\mathbf{b}_i$ can be written as $\mathbf{a}_i = [a_{ix}, a_{iy}, 0]^T$ and $\mathbf{b}_i = [b_{ix}, b_{iy}, 0]^T$, where a_{ix}, a_{iy}, b_{ix} and b_{iy} are design parameters related to the radii r and R of the moving platform and the base. The above equations assume that points A_i lie in one horizontal plane, and points B_i lie in a lower horizontal plane. Assuming massless straight cables and using the Newton-Euler approach to determine the static model of the mechanism yields

$$\mathbf{M}\mathbf{t} = \mathbf{g} \tag{2}$$

where $\mathbf{M}$ is the Jacobian matrix of the mechanism, whose expression is written as

$$\mathbf{M} = \begin{bmatrix} \boldsymbol{\rho}_1 & \boldsymbol{\rho}_2 & \boldsymbol{\rho}_3 & \boldsymbol{\rho}_4 & \boldsymbol{\rho}_5 & \boldsymbol{\rho}_6 \\ \boldsymbol{\rho}_1 \times \mathbf{b}_1 & \boldsymbol{\rho}_2 \times \mathbf{b}_2 & \boldsymbol{\rho}_3 \times \mathbf{b}_3 & \boldsymbol{\rho}_4 \times \mathbf{b}_4 & \boldsymbol{\rho}_5 \times \mathbf{b}_5 & \boldsymbol{\rho}_6 \times \mathbf{b}_6 \end{bmatrix}. \tag{3}$$

Parameter $\mathbf{t}$ is the vector containing the tensions in the cables per unit cable length and per unit platform mass and $\mathbf{g}$ the load wrench per unit platform mass, which is the external force applied on the effector. Their expressions are given as

$$\mathbf{t} = [t_1, t_2, t_3, t_4, t_5, t_6]^T, \qquad \mathbf{g} = [0, 0, g, 0, 0, 0]^T \tag{4}$$

where g is the gravitational acceleration and where it is assumed that the centre of mass of the platform is located at point $\mathbf{p}$, i.e., the centre of the platform.

3.2 Determination of the Static Workspace

The static workspace under constant orientation is now determined analytically based on Eq. 2. The static workspace corresponds to all the positions of the moving platform for which the tension of the cables are all positive. Moreover, the Jacobian matrix $\mathbf{M}$ can be simplified since the orientation of the platform is constant. First, the cross product $\boldsymbol{\rho}_i \times \mathbf{b}_i$ is computed as

$$\boldsymbol{\rho}_i \times \mathbf{b}_i = [\ -zb_{iy},\ zb_{ix},\ b_{iy}\,(x - a_{ix}) - b_{ix}\,(y - a_{iy})\ ]^T. \tag{5}$$

Therefore, Eq. (2) can be rewritten as

$$\begin{bmatrix} x + b_{1x} - a_{1x} & \dots \\ y + b_{1y} - a_{1y} & \dots \\ z & \dots \\ -zb_{1y} & \dots \\ zb_{1x} & \dots \\ b_{1y}\,(x - a_{1x}) - b_{1x}\,(y - a_{1y}) & \dots \end{bmatrix} \begin{bmatrix} t_1 \\ t_2 \\ t_3 \\ t_4 \\ t_5 \\ t_6 \end{bmatrix} = \begin{bmatrix} 0 & \text{(I)} \\ 0 & \text{(II)} \\ g & \text{(III)} \\ 0 & \text{(IV)} \\ 0 & \text{(V)} \\ 0 & \text{(VI)} \end{bmatrix}. \tag{6}$$

Factoring out z in Eqs. (IV) and (V) yields the following expressions

$$b_{1y}t_1 + b_{2y}t_2 + b_{3y}t_3 + b_{4y}t_4 + b_{5y}t_5 + b_{6y}t_6 = 0 \tag{7}$$

$$b_{1x}t_1 + b_{2x}t_2 + b_{3x}t_3 + b_{4x}t_4 + b_{5x}t_5 + b_{6x}t_6 = 0 \tag{8}$$

which can then be used to simplify Eqs. (I), (II), (VI) since the sums introduced by Eqs. (7) and (8) appear in these equations. Thus, the system of Eq. (6) can be rewritten as

$$\begin{bmatrix} x - a_{1x} & x - a_{2x} & x - a_{3x} & x - a_{4x} & x - a_{5x} & x - a_{6x} \\ y - a_{1y} & y - a_{2y} & y - a_{3y} & y - a_{4y} & y - a_{5y} & y - a_{6y} \\ z & z & z & z & z & z \\ b_{1y} & b_{2y} & b_{3y} & b_{4y} & b_{5y} & b_{6y} \\ b_{1x} & b_{2x} & b_{3x} & b_{4x} & b_{5x} & b_{6x} \\ c_1 & c_2 & c_3 & c_4 & c_5 & c_6 \end{bmatrix} \begin{bmatrix} t_1 \\ t_2 \\ t_3 \\ t_4 \\ t_5 \\ t_6 \end{bmatrix} = \begin{bmatrix} 0 \\ 0 \\ g \\ 0 \\ 0 \\ 0 \end{bmatrix} \tag{9}$$

with

$$c_i = b_{ix}a_{iy} - a_{ix}b_{iy}, \qquad i = 1, \dots, 6 \tag{10}$$

which corresponds to the last component of the cross product $\mathbf{b}_i \times \mathbf{a}_i$. It can be observed that, as expected, the Jacobian matrix $\mathbf{M}$ is singular for $z = 0$, which occurs when the position of the reference point of the platform is in the plane defined by the fixed base. A potential boundary of the static workspace is found when one of the cable tensions is equal to zero. Setting one tension t_i to zero in Eq. (9) deletes the i-th column of the Jacobian matrix $\mathbf{M}$ and the i-th component of vector $\mathbf{t}$, which are denoted, respectively, matrix $\mathbf{M}_i$ with six rows

and five columns and vector $\mathbf{t}_i$, which contains the remaining five tensions. The resulting system of equations is

$$\mathbf{M}_{i\ [6\times5]}\mathbf{t}_{i\ [5\times1]} = \mathbf{g}. \tag{11}$$

Then, one can define the i-th augmented matrix $\mathbf{M}_{a-i}$ based on matrix $\mathbf{M}_i$ and the wrench load $\mathbf{g}$, namely

$$\mathbf{M}_{a-i} = \left[\mathbf{M}_i \mid \mathbf{g}\right] \tag{12}$$

which is a six-by-six matrix. For Eq. (11) to have a solution, vector $\mathbf{g}$ must be in the range of matrix $\mathbf{M}_i$, i.e., vector $\mathbf{g}$ must not be independent from the columns of $\mathbf{M}_i$. Therefore, the over-determined system in Eq. (11) yields a solution if the augmented matrix $\mathbf{M}_{a-i}$ has linearly dependent columns, which occurs when its determinant is zero, namely

$$\det\left(\mathbf{M}_{a-i}\right) = 0. \tag{13}$$

Equation (13) provides the positions $[x, y, z]$ where the tension of the i-th cable is zero, which corresponds to a potential limit of the static workspace. By inspection of Eq. (9), one can notice that expanding the determinant of Eq. (13) using the pivot placed on the third row and the last column of the augmented matrix $\mathbf{M}_{a-i}$ factors out variables g and z, which can then be eliminated because the determinant is set to 0. Thus, the static workspace of the effector for constant orientation is independent from the z coordinate of the platform and from the magnitude of the gravitational load. Moreover, subtracting the first column from columns 2 to 5 of the determinant of matrix $\mathbf{M}_{a-i}$ and expanding the determinant leads to the scalar equation

$$G_i x + H_i y + K_i = 0 \tag{14}$$

where coefficients G_i, H_i and K_i are functions of the architectural parameters of the mechanism only, defined by the components of vectors $\mathbf{a}_i$ and $\mathbf{b}_i$. Setting each cable tension to zero yields equations for six lines in the horizontal plane that define six half-planes when projected perpendicularly to the horizontal plane. The intersection of these six half-planes constitutes the static equilibrium workspace.

3.3 Application to a Three-DOF Cable-Suspended Mechanism with Crossing Cables

The architecture with crossing cables has particular properties that further simplify the system of equations presented in Eq. (9). First, one can define one pair of cables with vectors $\mathbf{a}_1$, $\mathbf{a}_2$, $\mathbf{b}_1$, $\mathbf{b}_2$ as shown in Fig. 4 and assume that the other two pairs are obtained with rotations of $\pm 2\pi/3$ around the centre of the base, referred to as the rotation matrices $\mathbf{Q}_1$ and $\mathbf{Q}_2$. For the particular architecture

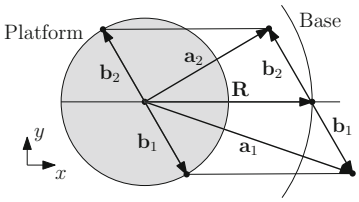

Fig. 4. Details of the architecture with crossing cables. The base lies in the plane $z = 0$ and the platform lies in a parallel plane at the z-coordinate of position vector $\mathbf{p}$, as defined in Fig. 3.

with crossing cables, the expressions for vectors $\mathbf{a}_1$ and $\mathbf{a}_2$ can be simplified as follows

$$\mathbf{a}_1 = \mathbf{R} + \mathbf{b}_1, \quad \mathbf{a}_2 = \mathbf{R} + \mathbf{b}_2 \tag{15}$$

where $\mathbf{R} = [R, 0, 0]^T$ is the position vector from the origin of the base frame to the midpoint of the line segment joining the attachment points on the base for the first pair of cables. Thus, the expressions for $\boldsymbol{\rho}_1, \ldots, \boldsymbol{\rho}_6$ from Eq. 1 become

$$\boldsymbol{\rho}_1 = \boldsymbol{\rho}_2 = \mathbf{p} - \mathbf{R}, \quad \boldsymbol{\rho}_3 = \boldsymbol{\rho}_4 = \mathbf{p} - \mathbf{Q}_1\mathbf{R}, \quad \boldsymbol{\rho}_5 = \boldsymbol{\rho}_6 = \mathbf{p} - \mathbf{Q}_2\mathbf{R}. \tag{16}$$

Moreover, the expression of the coefficients c_i in Eq. (9) is obtained from the last component of the cross product $\mathbf{b}_i \times \mathbf{a}_i$, whose expression can be written as

$$[\mathbf{b}_1 \times \mathbf{a}_1]_z = [\underbrace{\mathbf{Q}_1\mathbf{b}_1 \times \mathbf{Q}_1\mathbf{a}_1}_{\mathbf{b}_3 \times \mathbf{a}_3}]_z = [\underbrace{\mathbf{Q}_2\mathbf{b}_1 \times \mathbf{Q}_2\mathbf{a}_1}_{\mathbf{b}_5 \times \mathbf{a}_5}]_z = [\mathbf{b}_1 \times \mathbf{R}]_z = -Rb_{1y}, \tag{17}$$

$$[\mathbf{b}_2 \times \mathbf{a}_2]_z = [\underbrace{\mathbf{Q}_1\mathbf{b}_2 \times \mathbf{Q}_1\mathbf{a}_2}_{\mathbf{b}_4 \times \mathbf{a}_4}]_z = [\underbrace{\mathbf{Q}_2\mathbf{b}_2 \times \mathbf{Q}_2\mathbf{a}_2}_{\mathbf{b}_6 \times \mathbf{a}_6}]_z = [\mathbf{b}_2 \times \mathbf{R}]_z = -Rb_{2y}. \tag{18}$$

The results given in Eqs. (17) and (18) are obtained based on the fact that rotations $\mathbf{Q}_1$ and $\mathbf{Q}_2$ are performed in the same plane as vectors $\mathbf{b}_i$ and $\mathbf{R}$ and that the cross product is invariant to rotations performed in the plane defined by the two vectors to be multiplied. Using parameters $\mathbf{b}_i$ defined in Table 1 for the architecture with crossing cables, parameter r can be factored out from Eq. (9), which can then be further simplified after linear combinations among the last three rows, to become

$$\begin{bmatrix} x-R & x-R & x+\frac{1}{2}R & x+\frac{1}{2}R & x+\frac{1}{2}R & x+\frac{1}{2}R \\ y & y & y-\frac{\sqrt{3}}{2}R & y-\frac{\sqrt{3}}{2}R & y+\frac{\sqrt{3}}{2}R & y+\frac{\sqrt{3}}{2}R \\ z & z & z & z & z & z \\ 1 & -1 & 0 & 0 & 0 & 0 \\ 0 & 0 & 1 & -1 & 0 & 0 \\ 0 & 0 & 0 & 0 & 1 & -1 \end{bmatrix} \begin{bmatrix} t_1 \\ t_2 \\ t_3 \\ t_4 \\ t_5 \\ t_6 \end{bmatrix} = \begin{bmatrix} 0 \\ 0 \\ g \\ 0 \\ 0 \\ 0 \end{bmatrix}. \tag{19}$$

Expanding the determinant of the six augmented matrices $\mathbf{M}_{a-i}$ yields the three equations

$$x - R - \sqrt{3}y = 0, \qquad x - R + \sqrt{3}y = 0, \qquad x + \frac{1}{2}R = 0. \tag{20}$$

The equations for each cable in a given pair in Eq. (19) describe the same half plane, with the three half-planes then enclosing a triangular-prism-shaped volume. Furthermore, the static workspace of the architecture with crossing cables depends only on the radius R of the base frame and is independent from the size of the moving platform r.

4 Workspace Comparison for Cable-Suspended Parallel Mechanisms with Three Translational DOFs

The determination of the line equations that limit the static workspace for constant orientation is based on the calculation of the determinant of each augmented matrix $\mathbf{M}_{a-i}$, as shown in Subsect. 3.2. This method is now applied to different architectures for cable-suspended robots.

4.1 Mechanisms with Three DOFs

The analytical technique presented above is first applied to the two three-DOF architectures of Fig. 2. The static workspaces for both architectures, which are depicted with shaded areas, have triangular shapes, which means that the line equations that define the boundaries of the workspace are identical by pairs. For the trivial architecture, these equations are

$$x + \frac{1}{2}R - \frac{\sqrt{3}}{4}r - \sqrt{3}y = 0, \quad x + \frac{1}{2}R - \frac{\sqrt{3}}{4}r + \sqrt{3}y = 0, \quad x - \frac{1}{4}R + \frac{\sqrt{3}}{8}r = 0. \tag{21}$$

Figure 5 shows the static workspace delimited by the line equations of Eqs. (20) and (21), with unitary base radius R and platform radius $r = \frac{1}{2}R$. The static workspace for the trivial architecture shown in Fig. 5a is much smaller than that of the crossing-cables architecture shown in Fig. 5b. Indeed, crossing the cables over the mobile platform *significantly* increases the static workspace of the robot. The vertices of the static workspace for the crossing-cables architecture are located on the base circle of radius R, which represents an area about 12.5 times bigger than the area of the workspace of the trivial architecture.

4.2 Comparison with Six-DOF Architectures

Figure 6 shows the architecture and the workspace of a six-DOF cable mechanism actuated with six motors used for large-scale 3D printing [10] and for appearance modelling of objects [8]. This architecture is used as a reference for

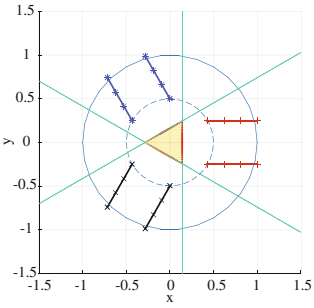

(a) Static workspace of the trivial architecture.

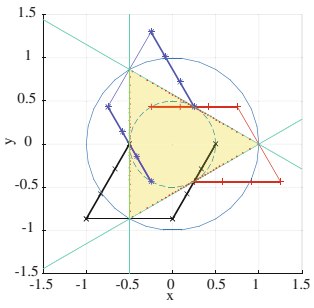

(b) Static workspace of the architecture with crossing cables.

Fig. 5. Static workspace of the centre point of the platform for two architectures of a three-DOF cable-suspended robot with parallelogram architecture. Distances in x and y are normalized by R, the radius of the base circle.

assessing the performance of the three-DOF cable-suspended architecture for translational motions proposed in this paper. The mobile platform for the six-DOF mechanism possesses three attachment points, with two cables connected to each, as shown in Fig. 6a. The line equations that define the static workspace for this mechanism are

$$x \pm R - \sqrt{3}y = 0, \quad x \pm R + \sqrt{3}y = 0, \quad x \pm \frac{1}{2}R = 0. \tag{22}$$

The resulting hexagonal-prism-shaped workspace, depicted in Fig. 6b, is contained inside the static workspace shown in Fig. 5b for the proposed three-DOF architecture, which is about 1.5 bigger. Thus, the proposed architecture, shown in Fig. 2b, is more effective at generating a large static workspace. However, one can notice that upper bounds on the cable tensions were not taken

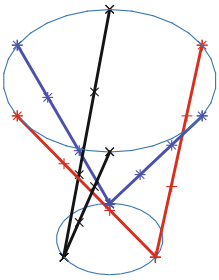

(a) Architecture of a six-DOF cable-suspended robot used for large-scale 3D printing [10].

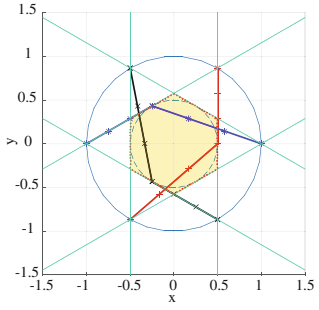

(b) Corresponding static workspace of the six-DOF robot, for the centre point of the platform.

Fig. 6. Architecture and static workspace of a six-DOF cable-suspended robot.

into consideration during the analysis. Indeed, for the proposed architecture, only three motors support the weight of the effector whereas the wrench load is distributed among the six actuators for the configuration in Fig. 6a. Also, the wrench load is assumed to be applied at the centre of mass of the platform, which might not be the case in a real application.

5 Conclusion

This paper proposes the design of a three-DOF translational cable-suspended mechanism whose cables are arranged as parallelograms with cables crossing over the moving platform. The main motivation of the work is to reduce the number of actuators needed in a translational parallel cable-suspended robot while ensuring a large workspace. One of the applications of such a mechanism is large-scale 3D printing, which typically requires positioning an end-effector with a constant orientation. One particular arrangement of the proposed architecture was described and its static equilibrium workspace was determined analytically and compared to that of a six-DOF cable-suspended robot. It was shown that the proposed architecture produces a larger translational workspace, therefore justifying its potential to replace the system actuated with six motors. Future work involves the evaluation of the kinematic sensitivity of the three-DOF mechanism as well as the development of a prototype for experimentally assessing its static workspace and thus its capabilities for 3D printing and/or other applications.

Acknowledgements. Comments provided by Xiaoling Jiang and Pascal Dion-Gauvin were much appreciated during the research. This work was supported by The Natural Sciences and Engineering Research Council of Canada (NSERC), by the Fonds de la Recherche du Québec sur la Nature et les Technologies (FRQNT) and by the Canada Research Chair Program.

References

1. Riechel, A.T., Ebert-Uphoff, I.: Force-feasible workspace analysis for underconstrained, point-mass cable robots. In: IEEE International Conference on Robotics and Automation, pp. 4956–4962 (2004)
2. Albus, J., Bostelman, R., Dagalakis, N.: The NIST robocrane. J. Robot. Syst. **10**(5), 709–724 (1993)
3. Pusey, J., Fattah, A., Agrawal, S., Messina, E.: Design and workspace analysis of a 6–6 cable-suspended parallel robot. Mech. Mach. Theory **39**(7), 761–778 (2004)
4. Perreault, S., Cardou, P., Gosselin, C.M., Otis, M.J.-D.: Geometric determination of the interference-free constant-orientation workspace of parallel cable-driven mechanisms. J. Mech. Robot. **2** (2010)
5. Bosscher, P., Ebert-Uphoff, I.: Wrench-based analysis of cable-driven robots. In: IEEE International Conference on Robotics and Automation, pp. 4950–4955 (2004)
6. Stump, E., Kumar, V.: Workspaces of cable-actuated parallel manipulators. J. Mech. Des. **128**(1), 159–167 (2006)

7. Gouttefarde, M., Merlet, J.P., Daney, D.: Wrench-feasible workspace of parallel cable-driven mechanisms. In: IEEE International Conference on Robotics and Automation, pp. 1492–1497 (2007)
8. Gosselin, C., Bouchard, S.: A gravity-powered mechanism for extending the workspace of a cable-driven parallel mechanism: application to the appearance modelling of objects. Int. J. Automat. Technol. **4**(4), 372–379 (2010)
9. Pott, A., Bruckmann, T., Mikelsons, L.: Closed-form force distribution for parallel wire robots. In: Computational Kinematics, pp. 25–34 (2009)
10. Barnett, E., Gosselin, C.: Large-scale 3D printing with A cable-suspended robot. Addit. Manufact. **7**, 27–44 (2015)
11. Bosscher, P., Williams, R.L., Tummino, M.: A concept for rapidlydeployable cable robot search and rescue systems. In: International Design Engineering Technical Conferences and Computers and Information in Engineering Conference, pp. 1–10 (2005)
12. Saber, O.: A spatial translational cable robot. J. Mech. Robot. **7**(3) (2015)
13. Alikhani, A., Behzadipour, S., Vanini, S.A.S., Alasty, A.: Workspace analysis of a three DOF cable-driven mechanism. J. Mech. Robot. **1**(4), 041005-1–041005-7 (2009)
14. Lefrançois, S., Gosselin, C.: Point-to-point motion control of a pendulumlike 3-DOF underactuated cable-driven robot. In: IEEE International Conference on Robotics and Automation, pp. 5187–5193 (2010)
15. Gouttefarde, M., Collard, J.F., Riehl, N., Baradat, C.: Geometry selection of a redundantly actuated cable-suspended parallel robot. IEEE Trans. Robot. **31**(2), 501–510 (2015)
16. Otis, M.J.-D., Perreault, S., Nguyen Dang, T.-L., Lambert, P., Gouttefarde, M., Laurendeau, D., Gosselin, C.M.: Determination and management of cable interferences between two 6-DOF foot platforms in a cable-driven locomotion interface. IEEE Trans. Syst. Man Cybern. Part A Syst. Hum. **39**(3), 528–544 (2009)